

Elasticity of a contact-line and avalanche-size distribution at depinning

Pierre Le Doussal and Kay Jörg Wiese

CNRS-Laboratoire de Physique Théorique de l'Ecole Normale Supérieure, 73231 Paris Cedex 05, France

(Received 14 March 2010; published 8 July 2010)

Motivated by recent experiments, we extend the Joanny-deGennes calculation of the elasticity of a contact line to an arbitrary contact angle and an arbitrary plate inclination in presence of gravity. This requires a diagonalization of the elastic modes around the nonlinear equilibrium profile, which is carried out exactly. We then make detailed predictions for the avalanche-size distribution at quasistatic depinning: we study how the universal (i.e., short-scale independent) rescaled size distribution and the ratio of moments of local to global avalanches depend on the precise form of the elastic kernel.

DOI: [10.1103/PhysRevE.82.011108](https://doi.org/10.1103/PhysRevE.82.011108)

PACS number(s): 68.35.Rh

I. INTRODUCTION

One of the theoretically best understood classes of disordered systems are elastic manifolds in presence of disorder. Examples include pinning and depinning of vortex-lattices [1,2], magnetic domain walls [3–5], contact-line experiments [6–12], earthquakes [13], and fracture [14,15].

Two universality classes exist in these systems: zero-temperature equilibrium, where the system finds its ground state; and depinning, i.e., a driven system where thermal activation plays no role. Here, we study the latter class.

The experimentally best accessible system is contact-line depinning, since the advance of the contact line can be filmed. This allows to make close contact to the theory. The theory in question is based on the functional renormalization group, as reviewed in [16]. The idea is that the central object of the theory is the disorder correlator, which evolves under renormalization, and acquires a cusp at the Larkin length, the scale beyond which disorder dominates over elasticity. From a theoretical point of view, the cusp had been questioned for some time, since it seemingly invalidates the renormalization group (RG) treatment on which it relies. Only recently, an exact relation has been derived to relate the disorder correlator to an experimentally observable quantity, namely the center of mass fluctuations of the elastic object, in our case the contact line [17,18]. This concept has been verified numerically [19,20], and finally experimentally for the contact-line dynamics near depinning [6]. The latter experiment was an important confirmation of the theory, but questions remained. Especially, it was concluded that the precise form of the elastic energy of the contact line matters, not only for the disorder correlator encoded in the center-of-mass fluctuation, but even more sensibly for the avalanche-size distribution. Thus, a detailed prediction for the former is needed. Surprisingly, a review of the literature reveals that this problem appears to have been treated only neglecting gravity [21] [34], or in presence of gravity only in the case where the equilibrium configuration of the interface is flat and horizontal, as for a vertical wall and a contact angle θ of 90° [22,23], see Figs. 1 and 2. In the latter case, the elastic energy as a function of the Fourier-transformed height profile h_q takes the form:

$$\mathcal{E}[h] = \frac{1}{2} \int \frac{dq}{2\pi} \epsilon_q |h_q|^2, \quad \epsilon_q = \gamma \sqrt{q^2 + \kappa^2}, \quad (1)$$

with κ the inverse capillary length, and up to terms of order h^3 . In other cases, interpolation formulas have been proposed [24].

There is numerical evidence [25] that the contact-line energy Eq. (1) does not correctly describe the shape of the contact line depinning from a single defect. Surprisingly, the form of ϵ_q as given by Eq. (1) seems not to have been questioned, rather the discrepancies were attributed to higher-order terms in h . The latter are indeed present [26–28], even for $\theta=90^\circ$ and a vertical wall ($\varphi=0$), but for small perturbations they are subdominant with respect to the dominant term Eq. (1).

In the first part of the present article (Sec. III) we show that for contact-angles leading to a nonflat profile as plotted in Fig. 1, or for an inclined wall in Fig. 2, the elastic energy Eq. (1) cannot be used, but must be replaced by the more general form

$$\frac{\epsilon_q}{\kappa\gamma} = \frac{\sin(\theta)\cos(\varphi)}{t} + \frac{(r^2 - 1)[t(r+t) + 1]\sin^2(\theta)}{t(r^2 + 3rt + 3t^2 - 1)}$$

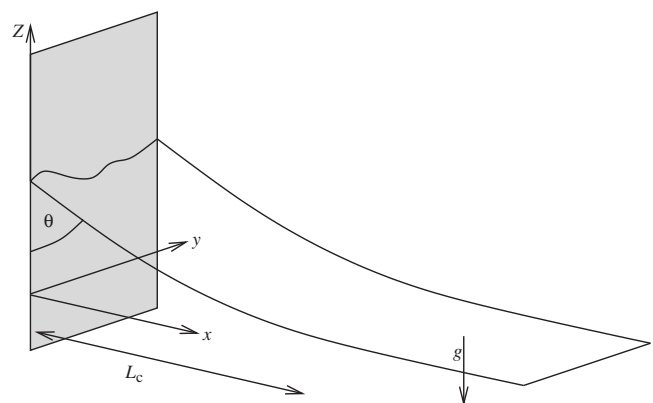


FIG. 1. The coordinate system for a vertical wall. The air/liquid interface becomes flat for $x \geq L_c$.

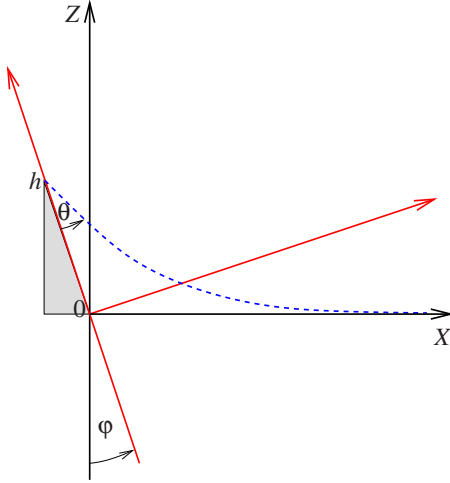


FIG. 2. (Color online) The coordinate system for a wall inclined by φ with respect to the vertical: the coordinate y , not shown, is perpendicular to the plane of the figure. The gray shaded volume is not filled by the liquid, leading to the gravity subtraction [second term in second-to-last line of Eq. (3)].

$$t = \sqrt{\frac{\sin(\theta + \varphi) + 1}{2}}, \quad r = \sqrt{1 + \frac{q^2}{\kappa^2}}. \quad (2)$$

This is plotted on Fig. 3. Then we discuss how this form can be measured from the contact line profile in presence of a single defect. This section is pedagogical and self-contained and can be read with no prior knowledge in either wetting or disordered systems.

In the second part of the paper (Sec. IV) we examine the consequences of the form Eq. (2) of the elastic kernel ϵ_q for the avalanche statistics of a contact-line at depinning, i.e., a contact-line advancing on a disordered substrate, when the fluid level is adiabatically increased. We calculate the local (i.e., at a given point) as well as global avalanche-size distribution, including the scaling functions. We work at quasi-static depinning using an over-damped equation of motion. The point of the present work is to study the effects arising from the precise form of the elastic kernel. We, therefore,

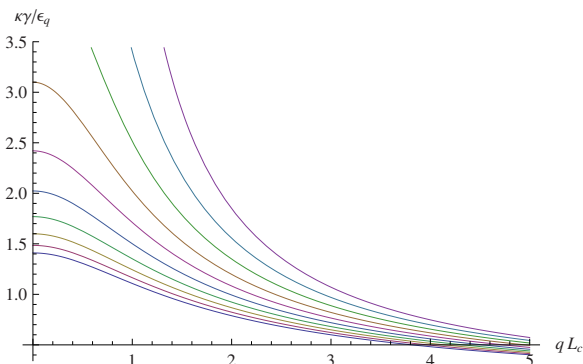


FIG. 3. (Color online) The height profile $z(x)$, in units of the capillary length L_c , for $\theta=30^\circ$ and $\varphi=0$. Different contact-angles $0 < \theta < \pi/2$ are obtained by moving the graph left/right. The case $\pi/2 < \theta < \pi$ is obtained by the reflection $z \rightarrow -z$.

assume that details of the dynamics as well as nonlinearities can be neglected in comparison. We use the methods introduced in [29] to compute the avalanche-size distribution from the functional renormalization group (FRG) theory of pinned elastic systems (see also Refs. [16] for a pedagogical introduction and [19,20] for early numerical tests of this theory). We recall and analyze the formula given in these references, hence this section can be read with no prior knowledge of disordered systems; however, understanding its foundations requires the knowledge of the above mentioned literature. Then we derive a general formula for the size distribution for an arbitrary elastic kernel, not given priorly, and compute universal ratios of local-avalanche-size moments versus global ones. Finally, we apply our general result to the contact line with the elasticity Eq. (2).

II. MODEL

Consider a fluid in a semi-infinite reservoir, bounded by a planar plate, in presence of gravity. The plate is inclined by an angle $-\pi/2 < \varphi < \pi/2$ with respect to the vertical, see Fig. 2. We consider the coordinate system X, y, Z where Z is along the vertical direction, and the equation of the plate is $Z = -X \cot \varphi$. The contact line of the fluid is parameterized by $[h(y), y]$ along the plate, hence it is at $[X = -h(y) \sin \varphi, y, Z = h(y) \cos \varphi]$ in our coordinate system. The fluid occupies the space $Z < Z(X, y)$ and $X > -Z \tan \varphi$, hence also $X > -h(y) \sin \varphi$, where $Z(X, y)$ is the height of the fluid-air surface. We choose the coordinate Z so that the reservoir level is $Z=0$ hence $Z(X \rightarrow \infty, y) = 0$.

The energy E is the sum of the fluid-air interface energy, proportional to the area, and the gravitational energy. It is a functional of $Z(X, y)$, with explicit dependence on $h(y)$. Its full expression reads:

$$\begin{aligned} \mathcal{E}[Z, h] &:= \frac{E[Z, h]}{\gamma} \\ &= \int dy \int_{X > -h(y) \sin \varphi} dX \left[\sqrt{1 + [\partial_X Z]^2 + [\partial_y Z]^2} + \frac{1}{2} \kappa^2 Z^2 \right] \\ &\quad - \frac{1}{2} \kappa^2 \int dy \int_{-h(y) \sin \varphi}^0 dX X^2 \cot^2 \varphi \\ &\quad - \int dy \int_{X > 0} dX 1 - \cos \theta \int dy h(y). \end{aligned} \quad (3)$$

γ is the surface tension, and

$$\kappa = \frac{1}{L_c} = \sqrt{\frac{\rho g}{\gamma}} \quad (4)$$

defines the capillary length L_c . We call \mathcal{E} the reduced energy. The first term is the area of the fluid surface; the second is the gravitational cost in potential energy for bringing a fluid element from infinity at level $Z=0$, filling the reservoir up to height $Z(X, y)$. The second line takes into account that for $\varphi > 0$ and $h(y) > 0$ (resp. $\varphi < 0$ and $h(y) < 0$) the volume element $0 < Z < -X \cot \varphi$ (respectively, $-X \cot \varphi < Z < 0$) is actually not filled by the liquid; this is the gray shaded region

on Fig. 2. Similarly for $\varphi > 0$ and $h(y) < 0$ [respectively, $\varphi < 0$ and $h(y) > 0$] there is a corresponding missing volume element which must be added. The third line is the subtraction of the surface energy of the flat profile $h(y)=0$ (i.e., $Z=0$ and $X>0$), necessary to make the problem well-defined. The last term comes from the difference between solid-fluid γ_{SF} and solid-air γ_{SA} surface energies which defines the *equilibrium* contact angle, denoted θ , via the usual relation $\gamma \cos \theta = \gamma_{SA} - \gamma_{SF}$. The definition of the contact line implies the additional boundary condition

$$Z(-h(y)\sin \varphi, y) = h(y)\cos \varphi. \quad (5)$$

The energy of a given configuration $h(y)$ of the contact line is obtained as $E[h] := E[Z_h, h]$ where $Z_h(X, y)$ minimizes $\mathcal{E}[Z, h]$ at fixed $h(y)$ under the constraint Eq. (5). By translational invariance, the minimum-energy configuration of the contact-line itself, i.e., the minimum of $E[h]$, is attained for a straight line $h(y)=h_0$ where h_0 denotes the equilibrium height.

In the next Section we compute the elastic energy of the contact line, i.e., $E[h]$ to second order in its deformations, i.e., $E[h] - E[h_0] = E_{el}[h] + \mathcal{O}(h^3)$ with

$$E_{el}[h] = \frac{1}{2} \int_q \epsilon_q h_{-q} h_q. \quad (6)$$

Here $h(y) = \int_q h_q e^{iqy}$ and we denote $\int_q := \int \frac{dq}{2\pi}$. For a uniform deformation $h(y)=h$ it takes the form:

$$\begin{aligned} \mathcal{E}[z, h] = & \int_{X > -h(y)\sin \varphi} dy \int_{x > x_0} dx \left[\frac{\kappa^2}{2} z(x, y)^2 - 1 + \sqrt{1 + [\partial_x z(x, y)]^2 + [\partial_y z(x, y) + \tilde{h}'(y)\sin \varphi \partial_x z(x, y)]^2} \right] \\ & - \frac{\kappa^2}{6} \cos^2 \varphi \sin \varphi \int dy h(y)^3 + (\sin \varphi - \cos \theta) \int dy h(y). \end{aligned} \quad (13)$$

To derive this result, we have used the relation

$$\begin{aligned} & \int_{X > -h(y)\sin \varphi} dX \sqrt{1 + [\partial_X Z]^2 + [\partial_Y Z]^2} - \int_{X > 0} dX 1 \\ & = h(y)\sin \varphi + \int_{X > -h(y)\sin \varphi} dX \sqrt{1 + [\partial_X Z]^2 + [\partial_Y Z]^2} - 1, \end{aligned}$$

which was then rewritten in terms of x .

The new height function obeys the constraint

$$z(x_0, y) = h(y)\cos \varphi, \quad (14)$$

i.e., it is specified on the edge $x=x_0$.

$$E_{el}[h] = \frac{1}{2} m^2 (h - h_0)^2 L_y, \quad m^2 = \epsilon_{q=0}, \quad (7)$$

which defines what we call the mass m , i.e., m^2 is the curvature of the parabolic well in which the contact line sits because of gravity [35]. We then calculate ϵ_q , already announced in Eq. (2).

III. CONTACT-LINE ELASTICITY

A. Model in shifted coordinates

We start by introducing a more convenient expression for the energy of the system. The constraint $X > -h(y)\sin \varphi$ in the domain of integration is tedious to handle, so we introduce the function $z(x, y)$ as

$$z(x, y) := Z(X = x - \tilde{h}(y)\sin \varphi, y). \quad (8)$$

It satisfies the same boundary condition $z(\infty, 0)=0$. We have also defined

$$\tilde{h}(y) := h(y) - h_0, \quad (9)$$

i.e., z is still the height along the vertical axis, but we have shifted the X coordinate so that the integration domain is

$$x > x_0 := -h_0 \sin \varphi. \quad (10)$$

Using that the derivatives, evaluated at $X = x - \tilde{h}(y)\sin \varphi$, satisfy

$$\partial_X Z(X, y) = \partial_x z(x, y) \quad (11)$$

$$\partial_Y Z(X, y) = \partial_y z(x, y) + \tilde{h}'(y)\sin \varphi \partial_x z(x, y), \quad (12)$$

one finds that the energy is now a functional noted $E[z, h] = \gamma \mathcal{E}[z, h]$ of $z(x, y)$ and $h(y)$ with

B. Zero mode and calculation of the mass

Let us first consider a uniform displacement of the line $h(y)=h$. We can then restrict to y -independent height functions $z(x, y)=z(x)$, and the reduced energy takes the form

$$\begin{aligned} L_y^{-1} \mathcal{E}[z, h] = & \int_{x > x_0} \left[\sqrt{1 + z'(x)^2} - 1 + \frac{\kappa^2}{2} z(x)^2 \right] \\ & - \frac{\kappa^2}{6} h^3 \cos^2 \varphi \sin \varphi + h(\sin \varphi - \cos \theta). \end{aligned} \quad (15)$$

There are additional constraints at the boundary,

$$z(x=x_0) = h \cos \varphi, \quad (16)$$

and $z=0$ at infinity. h is arbitrary and not necessarily the preferred value at equilibrium noted h_0 .

The linear variation of the reduced functional $\mathcal{E}[z, h]$ around an arbitrary configuration $(z(x), h)$, by $(\delta z(x), \delta h)$ can be written upon integration by part as

$$\begin{aligned} \delta \mathcal{E}[z, h]/L_y = & \int_{x>x_0} \delta z(x) \left[\kappa^2 z(x) - \partial_x \frac{z'(x)}{\sqrt{1+z'(x)^2}} \right] \\ & + \delta z(x_0) \cos[\theta(x_0) + \varphi] - \frac{\kappa^2}{2} \cos^2 \varphi \sin \varphi h^2 \delta h \\ & + \delta h (\sin \varphi - \cos \theta). \end{aligned} \quad (17)$$

We have defined

$$\cos(\theta(x) + \varphi) = -\frac{z'(x)}{\sqrt{1+z'(x)^2}} \quad (18)$$

$$\sin(\theta(x) + \varphi) = \frac{1}{\sqrt{1+z'(x)^2}}; \quad (19)$$

Hence, $\theta(x_0)$ is the contact angle at the wall and $\theta(x) + \varphi$ is the local angle with respect to the vertical. Note that, because of $\kappa^2 > 0$, the profile decays and the boundary term at infinity does not contribute. The constraint on the boundary implies the additional relation

$$\delta z(x_0) = \delta h \cos \varphi. \quad (20)$$

Consider now the function $z(x) = z_h(x)$ which minimizes the energy at fixed h , i.e., $\delta h = 0$ and $\delta z(x_0) = 0$. This leaves the variations in the bulk, given in the first line of Eq. (17), leading to the stationarity condition

$$\kappa^2 z(x) = \frac{z''(x)}{(1+z'(x)^2)^{3/2}}. \quad (21)$$

It can be integrated once,

$$\frac{\kappa^2}{2} z(x)^2 = 1 - \frac{1}{\sqrt{1+z'(x)^2}}, \quad (22)$$

where the integration constant was fixed by considering the limit of $x \rightarrow \infty$. This yields at $x = x_0$,

$$\begin{aligned} \frac{\kappa^2}{2} h^2 \cos^2 \varphi = & 1 - \sin(\theta(x_0) + \varphi) \\ = & 2 \sin^2 \left(\frac{\theta(x_0)}{2} + \frac{\varphi}{2} - \pi/4 \right), \end{aligned} \quad (23)$$

using that $1 - \sin x = 2 \sin^2(x/2 - \pi/4)$. The sign of the root $h \cos \varphi$ must be opposite to the sign of $\theta(x_0) + \varphi - \pi/2$, and similarly when solving for z in Eq. (22). This yields

$$h \cos \varphi = -2L_c \sin \left(\frac{1}{2} \left[\theta(x_0) + \varphi - \frac{\pi}{2} \right] \right). \quad (24)$$

Integrating once more, we obtain the height profile $z = z_h(x)$ in the inverse form, plotted on Fig. 4

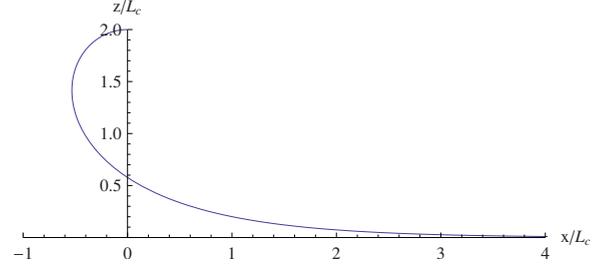


FIG. 4. (Color online) $\kappa\gamma/\epsilon_q$ as a function of qL_c , for $\theta=40^\circ$, $\varphi=0^\circ, 10^\circ, \dots, 90^\circ$ (from bottom to top).

$$\begin{aligned} x(z) = & x_0 + L_c \left[\operatorname{arcosh} \left(\frac{2L_c}{z} \right) - \operatorname{arcosh} \left(\frac{2L_c}{h \cos \varphi} \right) \right] \\ & - L_c \left(\sqrt{4 - \frac{z^2}{L_c^2}} - \sqrt{4 - \frac{h^2 \cos^2 \varphi}{L_c^2}} \right). \end{aligned} \quad (25)$$

The integration constant was chosen to satisfy the constraint Eq. (16).

The reduced energy of the uniform deformation $h(y) = h$ is thus a simple function $\mathcal{E}(h) = \mathcal{E}[z_h, h]$, whose derivative, $\mathcal{E}'(h)$ is easy to obtain. Indeed we can use the general variational formula (17) around $(z_h(x), h)$ setting $\delta z(x) = \delta h \partial_h z_h(x)$ with $\partial_h z_h(x_0) = 1$ from the constraint Eq. (16). The bulk contribution is zero, due to the ‘‘equation of motion’’ Eq. (21) satisfied by $z_h(x)$. The boundary contributions, i.e., the second and third lines in Eq. (17), give

$$\begin{aligned} \mathcal{E}'(h)/L_y = & \cos \varphi \cos(\theta(x_0) + \varphi) \\ & - \frac{\kappa^2}{2} h^2 \cos^2 \varphi \sin \varphi + \sin \varphi - \cos \theta. \end{aligned} \quad (26)$$

Using Eq. (23) this simplifies to

$$\mathcal{E}'(h)/L_y = \cos \theta(x_0) - \cos \theta, \quad (27)$$

where $\theta(x_0)$ is an implicit function of h , using Eq. (24). We first note that this allows to recover the usual condition for equilibrium, $\mathcal{E}'(h_0) = 0$, namely, that the local contact angle $\theta(x_0) = \theta$, the equilibrium contact angle. The equation determining h_0 is thus (24), with $\theta(x_0) = \theta$,

$$h_0 \cos \varphi = -2L_c \sin \left(\frac{1}{2} \left(\theta + \varphi - \frac{\pi}{2} \right) \right). \quad (28)$$

Inverting Eq. (28) one finds from Eq. (27) away from equilibrium

$$\begin{aligned} \frac{\mathcal{E}'(h)}{L_y} = & h \kappa \cos^2 \varphi \sqrt{1 - \frac{1}{4} \kappa^2 h^2 \cos^2 \varphi} \\ & + \left(1 - \frac{1}{2} h^2 \kappa^2 \cos^2 \varphi \right) \sin \varphi - \cos \theta. \end{aligned} \quad (29)$$

The mass for the zero mode is thus, after various simplifications

$$m^2 = \frac{\gamma \mathcal{E}''(h_0)}{L_y} = \frac{\gamma \kappa \sqrt{2} \cos \varphi \sin \theta}{\sqrt{1 + \sin(\theta + \varphi)}}. \quad (30)$$

An interesting special case is that of a flat interface, $\theta + \varphi = \frac{\pi}{2}$. Then

$$m^2 = \gamma \kappa \sin^2(\theta). \quad (31)$$

C. Elastic energy for arbitrary deformations

We now go back to the general case for $h(y)$. The reduced energy functional $\mathcal{E}[z, h]$ given in Eq. (13) explicitly depends on $h(y)$. In addition $h(y)$ also enters in the boundary condition Eq. (14). It is important to distinguish these two dependencies, which render the calculation a little tedious. The reader only interested in the results can proceed directly to Eq. (61).

We call $z_h(x, y)$ the profile which minimizes the reduced energy functional $\mathcal{E}[z, h]$ with fixed $h(y)$, hence with respect to bulk variations $\delta z(x, y)$ only,

$$\frac{\delta \mathcal{E}}{\delta z(x, y)} \Big|_{\text{bulk}} [z_h, h] = 0, \quad (32)$$

i.e., a partial (functional) derivative with respect to z only.

We now expand around the equilibrium solution as follows:

$$\begin{aligned} h(y) &= h_0 + \tilde{h}(y) \\ z_h(x, y) &= z_0(x) + \tilde{z}(x, y), \end{aligned} \quad (33)$$

where $z_0(x) := z_{h_0}(x)$ is the equilibrium profile determined in the previous section. Since \tilde{z} is of order $\mathcal{O}(\tilde{h})$, to compute the elastic energy we need to expand the minimum energy to second order in \tilde{h} and \tilde{z} . Expanding Eq. (13) to second order in the *explicit* dependence on \tilde{z} and \tilde{h} we have

$$\begin{aligned} \mathcal{E}[z_h, h] - \mathcal{E}[z_0, h_0] &= \delta^{(1)}\mathcal{E} + \delta^{(2)}\mathcal{E} + \mathcal{O}(\tilde{h}^3) \\ \delta^{(2)}\mathcal{E} &= \delta^{(2,1)}\mathcal{E} + \delta^{(2,2)}\mathcal{E} + \delta^{(2,3)}\mathcal{E}. \end{aligned} \quad (34)$$

The first term is the linear variation,

$$\delta^{(1)}\mathcal{E} = \frac{\delta \mathcal{E}}{\delta z} [z_0, h_0] \cdot \tilde{z} + \frac{\delta \mathcal{E}}{\delta h} [z_0, h_0] \cdot \tilde{h}, \quad (35)$$

whereas $\delta^{(2,p)}\mathcal{E}$ are second order variations computed below. Let us start with $\delta^{(1)}\mathcal{E}$:

$$\begin{aligned} \delta^{(1)}\mathcal{E} &= \int_y \int_{x>x_0} \tilde{z}(x, y) \left[\kappa^2 z_0(x) - \partial_x \frac{z_0'(x)}{\sqrt{1 + z_0'(x)^2}} \right] \\ &+ \int_y \delta z(x_0, y) \cos(\theta(x_0) + \varphi) \\ &- \frac{\kappa^2}{2} \cos^2 \varphi \sin \varphi h_0^2 \int_y \tilde{h}(y) \\ &+ \int_y \tilde{h}(y) (\sin \varphi - \cos \theta). \end{aligned} \quad (36)$$

The first line is the bulk variation which vanishes since $z_0(x)$ satisfies the stationarity condition Eq. (21). The rest is the sum of the *boundary* variation in z and the variation in h . Thanks to the exact constraint

$$\tilde{z}(x_0, y) = \tilde{h}(y) \cos \varphi, \quad (37)$$

one can check, using the results of the previous section, that this sum vanishes identically if h_0 is the equilibrium value. Hence, we have $\delta^{(1)}\mathcal{E} = 0$. Since \tilde{z} also contains subdominant \tilde{h}^2 contributions, this is a quite useful observation, as we do not need to worry about them in computing the elastic energy. They drop out by virtue of the equilibrium condition.

Let us now study the three second variations. The first one is

$$\begin{aligned} \delta^{(2,1)}\mathcal{E} &= \frac{1}{2} \tilde{z} \cdot \frac{\delta^2 \mathcal{E}}{\delta z \delta z} [z_0, 0] \cdot \tilde{z} \\ &= \frac{1}{2} \int_{y, x>x_0} \kappa^2 \tilde{z}(x, y)^2 + \frac{[\partial_x \tilde{z}(x, y)]^2}{[1 + z_0'(x)^2]^{3/2}} \\ &+ \frac{[\partial_y \tilde{z}(x, y)]^2}{[1 + z_0'(x)^2]^{1/2}}. \end{aligned} \quad (38)$$

The second one is

$$\begin{aligned} \delta^{(2,2)}\mathcal{E} &= \tilde{h} \cdot \frac{\delta^2 \mathcal{E}}{\delta h \delta z} [z_0, h_0] \cdot \tilde{z} \\ &= \sin \varphi \int_{y, x>x_0} h'(y) \frac{z_0'(x)}{\sqrt{1 + z_0'(x)^2}} \partial_y \tilde{z}(x, y), \end{aligned} \quad (39)$$

where we have used $\tilde{h}'(y) = h'(y)$ to alleviate the notation. The third contribution is

$$\begin{aligned} \delta^{(2,3)}\mathcal{E} &= \frac{1}{2} \tilde{h} \cdot \frac{\delta^2 \mathcal{E}}{\delta h \delta h} [z_0, h_0] \cdot \tilde{h} \\ &= \delta^{(2,3a)}\mathcal{E} + \delta^{(2,3b)}\mathcal{E}, \end{aligned} \quad (40)$$

where we write separately the second derivative with respect to the explicit dependence on $\tilde{h}(y)$ of the surface energy, namely,

$$\delta^{(2,3a)}\mathcal{E} = \frac{1}{2} \sin^2 \varphi \int_y \int_{x>x_0} h'(y)^2 \frac{z_0'(x)^2}{\sqrt{1 + z_0'(x)^2}}, \quad (41)$$

and of the gravitational one,

$$\delta^{(2,3b)}\mathcal{E} = -\frac{1}{2} \kappa^2 \cos^2 \varphi \sin \varphi h_0 \int_y \tilde{h}(y)^2. \quad (42)$$

To compute the first two contributions one needs to specify the properties of $\tilde{z}(x, y)$ which follow from its definition Eq. (33). The function $z_h(x, y)$ must obey Eq. (32), for any h . Hence we can expand this equation order by order in h . For $h=0$ it yields again the stationarity condition Eq. (21) for $z_0(x)$; to first order it yields

$$\tilde{z} \cdot \frac{\delta \mathcal{E}}{\delta z \delta z(x,y)|_{\text{bulk}}} [z_0, h_0] + \tilde{h} \cdot \frac{\delta \mathcal{E}}{\delta h \delta z(x,y)|_{\text{bulk}}} [z_0, h_0] = 0,$$

which, in explicit form, yields the equation obeyed by $\tilde{z}(x, y)$ (to linear order in h which is all we need here):

$$\left\{ \kappa^2 - \partial_x \frac{1}{[1 + z_0'(x)^2]^{3/2}} \partial_x - \frac{1}{[1 + z_0'(x)^2]^{1/2}} \partial_y^2 \right\} \tilde{z}(x, y) = \sin \varphi h''(y) \frac{z_0'(x)}{[1 + z_0'(x)^2]^{1/2}}. \quad (43)$$

It must be solved with the boundary condition Eq. (37) and $\tilde{z}(x=\infty, y)=0$.

Remarkably, this complicated looking equation, which depends on the profile $z_0(x)$ known only in the implicit form Eq. (25), can be solved analytically. First of all, using the stationarity Eq. (21) satisfied by $z_0(x)$, one notes that

$$\tilde{z}(x, y) = \tilde{z}_1(x, y) := -\sin \varphi h(y) z_0'(x) \quad (44)$$

is a particular solution of (43) which vanishes at $x=\infty$ and takes the value

$$\tilde{z}_1(x_0, y) = \sin \varphi \cot(\theta + \varphi) h(y) \quad (45)$$

at the boundary. The full solution can thus be written as

$$\tilde{z}(x, y) = \tilde{z}_1(x, y) + \tilde{z}_2(x, y), \quad (46)$$

where $\tilde{z}_2(x, y)$ satisfies the homogeneous equation, i.e., Eq. (43) setting the r.h.s. to zero. The boundary condition Eq. (14) implies

$$\tilde{z}_2(x_0, y) = \frac{\sin \theta}{\sin(\theta + \varphi)} h(y). \quad (47)$$

Both \tilde{z}_1 and \tilde{z}_2 vanish at $x=\infty$.

To solve the homogeneous equation, we go to Fourier space in y direction, and introduce a new variable in x direction. We thus look for the solution in the form

$$\tilde{z}_2(x, y) = \frac{\sin \theta}{\sin(\theta + \varphi)} \int_q e^{iqy} \tilde{h}(q) F_{\tilde{q}}(S(x)), \quad (48)$$

$$S(x) = \sin(\theta(x) + \varphi) = \frac{1}{\sqrt{1 + z_0'(x)^2}}, \quad (49)$$

$$\tilde{q} = q/\kappa \quad (50)$$

with $S(x_0) = \sin(\theta + \varphi)$. Deriving Eq. (49) with respect to x , and using Eqs. (21) and (22) to express the result in terms of $S(x)$, we obtain the rule for changing the derivatives,

$$\partial_x = \kappa \frac{\sqrt{2(1-S)}\sqrt{S+1}}{S} \partial_S. \quad (51)$$

The resulting equation for the function $F_{\tilde{q}}(S)$ reads

$$\begin{aligned} & (\tilde{q}^2 S + 1) F_{\tilde{q}}(S) + (1-S)(7S^2 + S - 4) F_{\tilde{q}}'(S) \\ & - 2(S-1)^2 S(S+1) F_{\tilde{q}}''(S) = 0, \end{aligned} \quad (52)$$

where $\sin(\theta + \varphi) < S < 1$. The constraint Eq. (47) implies the

boundary conditions $F_{\tilde{q}}(\sin(\theta + \varphi)) = 1$ and $F_{\tilde{q}}(1) = 0$. After some search, the general solution of Eq. (52) which satisfies $F_{\tilde{q}}(1) = 0$ is found to be

$$F_{\tilde{q}}(S) = \frac{g_r(S)}{g_r(\sin(\theta + \varphi))} \quad (53)$$

$$\begin{aligned} g_r(S) &= \frac{(1-S)^{r/2}}{S} \left(1 + \frac{\sqrt{S+1}}{\sqrt{2}} \right)^{-r} \\ &\times (2r^2 + 3\sqrt{2}r\sqrt{S+1} + 3S + 1), \end{aligned} \quad (54)$$

where we denoted

$$r := \sqrt{1 + \tilde{q}^2}. \quad (55)$$

We now evaluate the second variation. Consider first the sum of Eqs. (38) and (39). Using the equation of motion Eq. (43) for \tilde{z} , the combination $\delta^{(2,1)} \mathcal{E} + \frac{1}{2} \delta^{(2,2)} \mathcal{E}$ can be integrated by part. Therefore, we obtain for the combination $[\delta^{(2,1)} \mathcal{E} + \frac{1}{2} \delta^{(2,2)} \mathcal{E}] + \frac{1}{2} \delta^{(2,2)} \mathcal{E}$

$$\begin{aligned} \delta^{(2,1)} \mathcal{E} + \delta^{(2,2)} \mathcal{E} &= -\frac{1}{2} \int_y \frac{\tilde{z}(x_0, y)}{[1 + z_0'(x)^2]^{3/2}} \partial_x \tilde{z}(x, y) \Big|_{x=x_0} \\ &- \frac{1}{2} \sin \varphi \int_{y, x > x_0} h''(y) \frac{z_0'(x)}{\sqrt{1 + z_0'(x)^2}} \tilde{z}(x, y). \end{aligned} \quad (56)$$

The last term has been integrated by part with respect to y [36]. To continue, we note the useful equality

$$\begin{aligned} & - \int_y \frac{\tilde{z}_1(x_0, y)}{[1 + z_0'(x)^2]^{3/2}} \partial_x \tilde{z}_2(x, y) \Big|_{x=x_0} \\ &= - \int_y \frac{\tilde{z}_2(x_0, y)}{[1 + z_0'(x)^2]^{3/2}} \partial_x \tilde{z}_1(x, y) \Big|_{x=x_0} \\ &+ \sin \varphi \int_{y, x > x_0} h''(y) \frac{z_0'(x)}{\sqrt{1 + z_0'(x)^2}} \tilde{z}_2(x, y), \end{aligned} \quad (57)$$

which is a consequence of the two different ways to integrate by part

$$\begin{aligned} & \int_{y, x > x_0} \left[\kappa^2 \tilde{z}_1(x, y) \tilde{z}_2(x, y) + \frac{[\partial_x \tilde{z}_2(x, y)][\partial_x \tilde{z}_1(x, y)]}{[1 + z_0'(x)^2]^{3/2}} \right. \\ & \left. + \frac{[\partial_y \tilde{z}_1(x, y)][\partial_y \tilde{z}_2(x, y)]}{[1 + z_0'(x)^2]^{1/2}} \right], \end{aligned}$$

and to use the equation of motion for \tilde{z}_1 (inhomogeneous) and \tilde{z}_2 (homogeneous).

Inserting $\tilde{z} = \tilde{z}_1 + \tilde{z}_2$ into Eq. (56) and using the equality Eq. (57) we get

$$\begin{aligned}
\delta^{(2,1)}\mathcal{E} + \delta^{(2,2)}\mathcal{E} = & -\frac{1}{2} \int_y \frac{\tilde{z}_2(x_0, y)}{[1 + z'_0(x)^2]^{3/2}} \partial_x \tilde{z}_2(x, y) \Big|_{x=x_0} \\
& -\frac{1}{2} \int_y \frac{\tilde{z}_1(x_0, y)}{[1 + z'_0(x)^2]^{3/2}} \partial_x \tilde{z}_1(x, y) \Big|_{x=x_0} \\
& - \int_y \frac{\tilde{z}_2(x_0, y)}{[1 + z'_0(x)^2]^{3/2}} \partial_x \tilde{z}_1(x, y) \Big|_{x=x_0} \\
& - \frac{1}{2} \sin \varphi \int_{y, x > x_0} h''(y) \frac{z'_0(x)}{\sqrt{1 + z'_0(x)^2}} \tilde{z}_1(x, y).
\end{aligned} \tag{58}$$

We now discuss simplifications. First, the last term in Eq. (58) exactly cancels $\delta\mathcal{E}^{(2,3a)}$; this is shown using Eq. (44).

Second, from Eqs. (44), (21), and (14), we obtain

$$\frac{\partial_x \tilde{z}_1(x, y)}{[1 + z'_0(x)^2]^{3/2}} \Big|_{x=x_0} = -\sin \varphi \cos \varphi \kappa^2 h(y) h_0. \tag{59}$$

This shows that the second line, half the third line and $\delta^{(2,3b)}\mathcal{E}$ cancel; the remaining half of the third line gives the first term reported in Eq. (60) below. The second term comes from the first line of Eq. (58), using Eq. (48), so we get finally:

$$\begin{aligned}
\delta^{(2)}\mathcal{E} = & \frac{\sin \varphi \cos \varphi \sin \theta}{2 \sin(\theta + \varphi)} \kappa^2 h_0 \int_y h(y)^2 \\
& - \frac{1}{2} \sin^2 \theta \sin(\theta + \varphi) \int_q h_q h_{-q} F_q(S(x)) \partial_x F_{-q}(S(x)) \Big|_{x=x_0}.
\end{aligned} \tag{60}$$

To compute the second term we use Eq. (51), where at the end S must be evaluated on the boundary $S = \sin(\theta + \varphi)$. To compute the first term we use the value Eq. (23) for h_0 .

This yields our final result for the elastic energy,

$$E_{\text{el}}[h] = \frac{1}{2} \int_q \epsilon_q h_q h_{-q}, \tag{61}$$

with

$$\begin{aligned}
\frac{\epsilon_q}{\kappa \gamma} = & \frac{\sin(\theta) \cos(\varphi)}{t} + \frac{(r^2 - 1)[t(r + t) + 1] \sin^2(\theta)}{t(r^2 + 3rt + 3t^2 - 1)} \\
t = & \sqrt{\frac{\sin(\theta + \varphi) + 1}{2}}, \quad r = \sqrt{1 + \frac{q^2}{\kappa^2}}.
\end{aligned} \tag{62}$$

One finds that ϵ_q is a scaling function of q/κ which reproduces formula (30) for the energy of a uniform mode $\epsilon_{q=0} = m^2$ as computed in the previous section, and which behaves as $\epsilon_q \approx \kappa \gamma \sin^2 \theta |q|$ for large $|q|$.

When $\varphi + \theta = \pi/2$, the equilibrium shape of the interface is flat. Thus the elastic energy is expected to simplify. Indeed, it becomes

$$\frac{\epsilon_q}{\kappa \gamma} = \sin^2(\theta) \sqrt{1 + \frac{q^2}{\kappa^2}}. \tag{63}$$

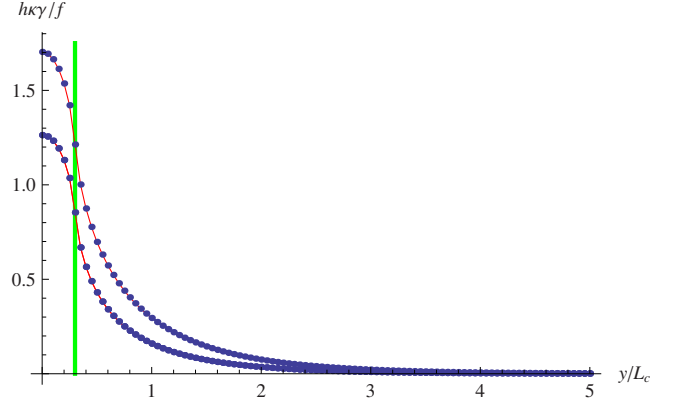


FIG. 5. (Color online) Sample profiles $h(y)$, in units of $f/(\kappa\gamma)$, plotted as a function of y/L_c , for $\theta=40^\circ$, $\varphi=0^\circ$ (bottom) and $\varphi=45^\circ$ (top). The profiles are the response to a force inside the green box $|y| < \delta = 0.3L_c$. The profile has to be continued symmetrically to the left.

D. Contact-line profile as a means of measuring ϵ_q

Suppose the contact line is in force-free equilibrium. Then pull on it with a force per unit length:

$$F(y) = \frac{f}{2\delta} \theta(|y| < \delta). \tag{64}$$

This leads in linear response (i.e., for the quadratic in h elastic energy we are using) to the following profile

$$h(y) = f \int_0^\infty \frac{dq \cos(qy) \sin(q\delta)}{\pi \epsilon_q q \delta}. \tag{65}$$

The limit of a δ -like force is recovered in the limit of $\delta \rightarrow 0$, which eliminates the last factor of $\sin(q\delta)/(q\delta)$. However the latter makes the integral convergent at large q . We have plotted for $\theta=40^\circ$ and $\delta=0.3$ two solutions on Fig. 5, one for $\varphi=0^\circ$ (bottom) and the other for $\varphi=45^\circ$ (top). We note that ϵ_q can be reconstructed from the profile as follows

$$\epsilon_q = f \frac{\sin(q\delta)}{q\delta} \left[2 \int_0^\infty dy \cos(qy) h(y) \right]^{-1}. \tag{66}$$

A reconstruction of ϵ_q starting from the blue points on the top of Fig. 5 is given in Fig. 6.

IV. AVALANCHE-SIZE DISTRIBUTIONS

A. Model

We now study the case of a disordered plate, which is immersed with velocity v into the liquid reservoir. This is the geometry of the experiment described in Ref. [6]. We use some of the notations defined there: x denotes the coordinate along the contact line (denoted y in the previous section) and $u(x)$ the height of the contact line along the plate, in the frame of the plate (Fig. 7). We reserve the notation $h(x)$ to the contact-line height measured in the laboratory frame, with the relation [37]:

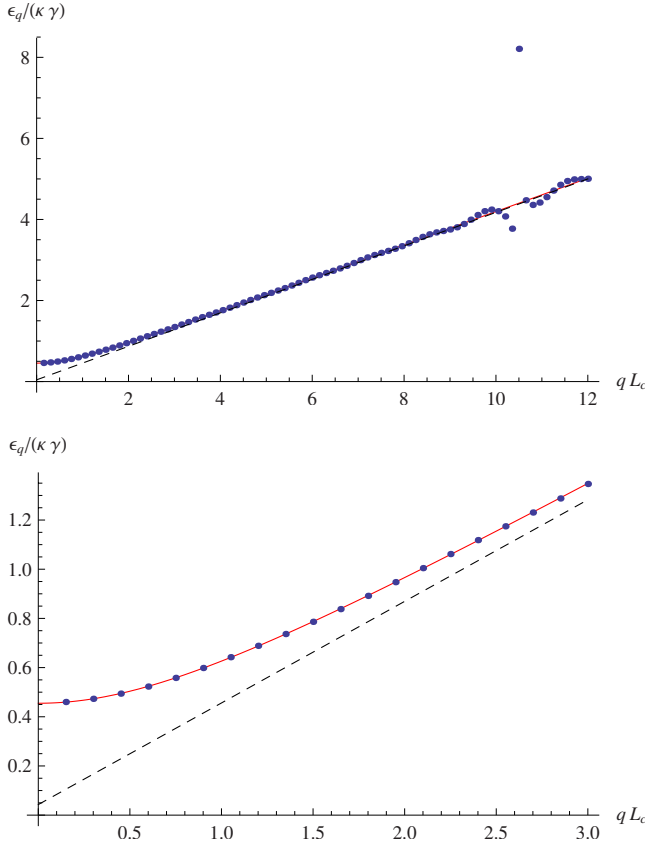


FIG. 6. (Color online) Top: Blue points: Reconstruction of ϵ_q , in units of $\kappa\gamma$, as a function of q/κ , using (66) from the points of the bottom curve of Fig. 5, i.e., a vertical plate geometry $\varphi=0$. Solid red line: the analytical result. One sees a numerical problem appearing at large q , at $q=\pi/\delta$, where δ is the box-size in Fig. 5. However, this is already far in the linear asymptotic regime (dashed line). Bottom: The same plot for smaller q . One sees that ϵ_q is well reconstructed.

$$h(x,t) = u(x,t) - w, \quad w = vt. \quad (67)$$

Even though it is a dynamical problem, it is useful to introduce the energy

$$\mathcal{H}[u] = \int_0^L dx \frac{m^2}{2} [u(x) - w]^2 + V(x, u(x)) + \delta E[u]. \quad (68)$$

Here m^2 is the mass of the zero mode $q=0$, and $\delta E[u] := \frac{1}{2} \int_q [\epsilon_q - \epsilon_0] u_q u_{-q}$ the remaining part of the elastic energy

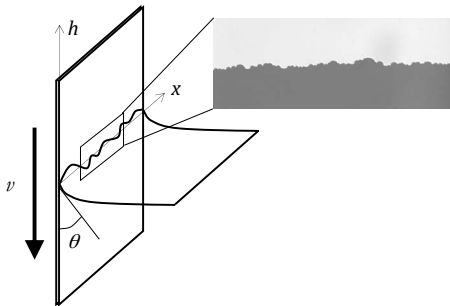


FIG. 7. Sketch of the experimental setup used in [6]. The size of the image in the inset is 1.5 mm.

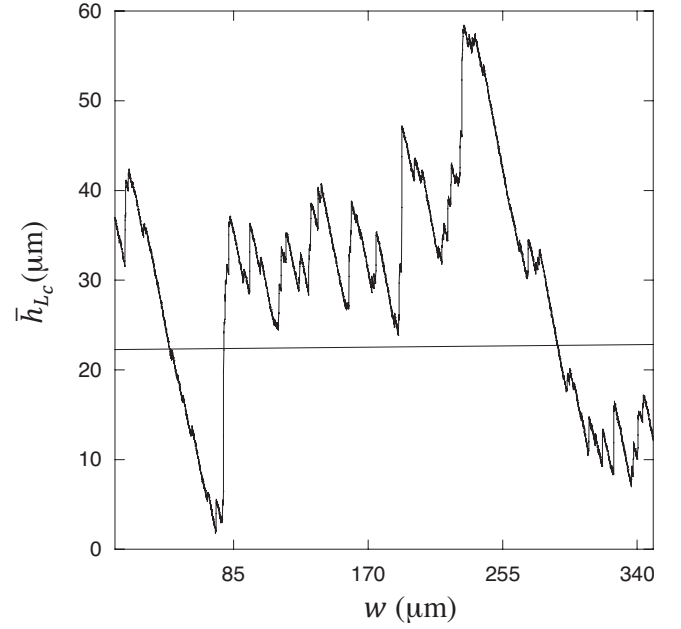


FIG. 8. Data from [6]: Height of the contact line $\bar{h}(w)$ averaged over $2L_c$, as a function of the position w of the plate (system: iso/Si). The fast depinning events (upwards) are clearly visible. Between them, the contact line moves downwards at the plate velocity v (here $1 \mu\text{m/s}$). The straight line is the reference level h_0 .

at nonzero wave vector $q \neq 0$. For the contact line, $m^2 = \epsilon_0$ and $\delta E[u]$ are both given in Eq. (62). We neglect possible nonlinear elastic terms [27,28]. The function $V(x, u)$ is a random potential, whose derivative $\partial_u V(x, u)$ is short-ranged correlated, modeling the disordered substrate.

The contact line is pinned by the disorder, but also trapped in the quadratic well with curvature m^2 . Advancing the well-position w by immersing the plate with velocity v leads to a motion of the contact line, which we now study in the quasistatic limit, i.e., the limit of small v . From the energy form Eq. (68) one can derive, upon various assumptions about the fluid, equations of motion (see e.g., [23,26] and references therein). Our assumption here is that in the quasistatic limit, they lead to the same statistics as the simplest over-damped model studied in Ref. [29], at least to the level of approximation that we use here (i.e., lowest order, i.e., one-loop FRG). Furthermore, although quasistatic dynamics and pure statics [38] are different, they lead, in the same order of approximation, to identical rescaled avalanche-size distributions. Deviations are expected only at the next, i.e., two-loop order. This justifies our studying of the energy form Eq. (68), and, as we will see, our point is that noticeable effects already arise from the precise form of the elastic kernel.

B. Global statistics of avalanches

1. Definitions

As can be seen on Fig. 8, the experiment [6] shows, as predicted by the theory [19,29], that the motion of the contact line proceeds by sudden jumps, i.e., avalanche motion.

For an avalanche occurring at a given position w of the center of the quadratic well, one defines $u_w^-(x)$ the contact-line position just before the avalanche and $u_w^+(x)$ its position just after. The size of the avalanche is defined as

$$S := \int_0^L dx [u_w^+(x) - u_w^-(x)] = \int_0^L dx [h_w^+(x) - h_w^-(x)]. \quad (69)$$

Hence one can measure the avalanche size S as the area swiped both in the u or in the h coordinate system.

We now recall the main results of Refs. [19,29] and apply the general formulation to various cases, including the contact line for which we have computed the elasticity in Sec.

III. The characteristic rescaled function $\tilde{Z}(\lambda)$ is defined as:

$$\tilde{Z}(\lambda) := \frac{S_m}{\langle S \rangle} \langle e^{\lambda S / S_m} - 1 \rangle \quad (70)$$

$$S_m := \frac{\langle S^2 \rangle}{2\langle S \rangle} = \frac{-\Delta'(0^+)}{m^4}. \quad (71)$$

All averages $\langle \dots \rangle$ are over the normalized probability density $P(S)$ of avalanches. By definition $\tilde{Z}(\lambda) = \lambda + \lambda^2 + \mathcal{O}(\lambda^3)$. The function $\Delta(w)$ is the renormalized correlator of the disorder defined and studied in [19,29] and measured in Ref. [6]. It is m dependent: at large m it is equal to the bare disorder correlator, while as m is decreased it develops a linear cusp at $u=0$, whose value, $\Delta'(0^+)$, is related to the second moment of the size distribution as displayed above in Eq. (71).

The scale S_m is the large-scale cutoff for avalanche sizes, originating from the quadratic well which suppresses the largest avalanches. It is an important scale as it allows to define universal functions in the limit where it becomes large, i.e., $S_m \gg S_{\min}$, where S_{\min} is the typical size of the smallest avalanches. In the variable $s := S/S_m$ the avalanche-size distribution becomes universal, especially the small- S behavior is expected to take a power-law form $P(S) \sim (\frac{S}{S_m})^{-\tau}$, with τ the avalanche-size exponent. Universal means independent of small-scale details, but not of the large-scale setting, e.g., it will depend on the precise form of the elastic kernel. Indeed, one of the predictions of the FRG theory is that if the exponent τ satisfies $2 > \tau > 1$ which will turn out to be the case here, then the distribution of avalanche sizes for $S \gg S_{\min}$ takes the form as $m \rightarrow 0$, i.e., $S_m \gg S_{\min}$,

$$P(S)dS := \frac{\langle S \rangle}{S_m} p\left(\frac{S}{S_m}\right) \frac{dS}{S_m}. \quad (72)$$

The function $p(s)$ is universal in the above sense. For a fixed elastic kernel it depends only on the space dimension d . Note that the normalized probability $P(S)$ depends on the cutoff S_{\min} via the first moment $\langle S \rangle$ which cannot be predicted by the theory, hence is an input from experiment. It is important to stress that while the function $p(s)$ is universal and convenient for data analysis, *it is not a probability distribution* and is not normalized to unity. Rather, it satisfies from its defini-

tion Eq. (72) and using Eq. (71) the two normalization conditions

$$\langle s \rangle_p = \int ds s p(s) = 1, \quad (73)$$

$$\langle s^2 \rangle_p = \int ds s^2 p(s) = 2. \quad (74)$$

Here and below we use the notation $\langle s \rangle_p$ to denote an integration over $p(s)$ and distinguish it from a true expectation value over $P(S)$, denoted $\langle \dots \rangle$. Note that $\tilde{Z}(\lambda)$ and $p(s)$ are related by the Laplace transform

$$\tilde{Z}(\lambda) = \int_0^\infty ds p(s) [e^{\lambda s} - 1]. \quad (75)$$

Note finally that the limit $m \rightarrow 0$ means that L_c is large compared to the microscopic cutoff a along the line, which may be of nanometer scale, or for strong disorder the size of the defects.

2. Results from one-loop FRG

We now summarize the results obtained in [29] for a general form of the elastic kernel ϵ_k . One defines:

$$\tilde{\epsilon}_k := \epsilon_k / \epsilon_0, \quad \epsilon_0 = m^2. \quad (76)$$

The general result of [29] is that $\tilde{Z}(\lambda)$ satisfies, in an expansion in powers of the renormalized disorder $\Delta(w)$ and up to terms of $\mathcal{O}(\Delta^2)$,

$$\tilde{Z} = \lambda + \tilde{Z}^2 + \alpha J(\tilde{Z}), \quad \alpha = -\epsilon \int_k \tilde{\epsilon}_k^{-2} \Delta''(0^+), \quad (77)$$

$$J(z) := \frac{1}{\epsilon \int_k \tilde{\epsilon}_k^{-2}} \int_k \left[\frac{z^2}{(\tilde{\epsilon}_k - 2z)^2} + \frac{z}{\tilde{\epsilon}_k - 2z} - \frac{z}{\tilde{\epsilon}_k} - 3 \frac{z^2}{\tilde{\epsilon}_k^2} \right]. \quad (78)$$

Note that the parameter

$$\epsilon := d_c - d, \quad (79)$$

the distance to the upper critical dimension, introduced here for later purpose, cancels and is thus immaterial in this formula. As such, this equation is formally exact for any m , any ϵ_k and any dimension, up to $\mathcal{O}(\Delta^2)$ terms.

Furthermore, consider now an elastic kernel such that:

$$\epsilon_k \sim_{k \rightarrow \infty} K k^\beta \quad (80)$$

with elasticity range $\beta \leq 2$ (i.e., long ranged for $\beta < 2$ and short-ranged for $\beta = 2$) and K the elastic constant. Assume that it takes the form

$$\tilde{\epsilon}_k = e(K^{1/\beta} k / \mu), \quad \mu^\beta := m^2, \quad (81)$$

where the elastic scaling function $e(p)$ is constructed as the unique dimensionless function of the dimensionless argument p which satisfies $e(0) = 1$, and $e(p) = p^\beta$ for $p \rightarrow \infty$.

Then, the result of [29] is that the formula (77) can be controlled, in the limit $m \rightarrow 0$ as an expansion in powers of $\epsilon = d_c - d$, where $d_c = 2\beta$ is the upper critical dimension. For this one uses that

$$\begin{aligned} \int_k \bar{\epsilon}_k^{-2} &= \mu^{d-2\beta} K^{-d/\beta} \int_p e(p)^{-2} \\ &= \mu^{-\epsilon} K^{-2+\epsilon/\beta} \frac{C_\beta}{\epsilon} + \mathcal{O}(1) \end{aligned} \quad (82)$$

in the limit $\epsilon = d_c - d \rightarrow 0$, where $C_\beta = 2(4\pi)^{-d_c/2} / \Gamma(\beta)$ is independent of the shape of the function $e(p)$. Since the one-loop FRG flow for Δ has the schematic form $-\mu \partial_\mu \Delta = -\mu \partial_\mu (\int_k \bar{\epsilon}_k^{-2}) \times \Delta^2 = (\epsilon \int_k \bar{\epsilon}_k^{-2}) \Delta^2$, it is convenient to introduce the rescaled disorder,

$$\tilde{\Delta}''(0^+) := \left(\epsilon \int_k \bar{\epsilon}_k^{-2} \right) \Delta''(0^+) = K^{-2} C_\beta \mu^{-\epsilon} \Delta''(0^+), \quad (83)$$

where the second equality holds to leading order in ϵ . This is precisely the parameter α defined above, i.e., $\alpha = -\tilde{\Delta}''(0)$. The one-loop FRG flow for the rescaled disorder admits a fixed point, from which one obtains, as $m \rightarrow 0$, that α flows to $\alpha = -\tilde{\Delta}''(0) = -\frac{1}{3}\epsilon(1 - \zeta_1)$. Here ζ_1 is the $\mathcal{O}(\epsilon)$ correction to the roughness exponent of the elastic object. For the type of disorder relevant for the contact line (i.e., random-field disorder) one has $\zeta_1 = 1/3$, hence

$$\alpha = -\frac{2}{9}\epsilon. \quad (84)$$

This value will be used from now on in Eq. (77), which is thus valid up to terms of order $\mathcal{O}(\epsilon^2)$. Using the above definitions one finds that to lowest order in ϵ , $J(z)$ depends only on the dimensionless scaling function $e(p)$, and not on the stiffness K :

$$J(z) = C_\beta^{-1} \int_p \left\{ \frac{z^2}{[e(p) - 2z]^2} + \frac{z}{e(p) - 2z} - \frac{z}{e(p)} - 3 \frac{z^2}{e(p)^2} \right\}, \quad (85)$$

valid for short range (SR) elasticity as well as LR elasticity. Of course, since we work to lowest order in ϵ , the above integral should be computed in the critical dimension $d = d_c$.

Note that the mean-field singularity of this equation corresponds to $p = 0$, $e(p = 0) = 1$, i.e., $z = 1/2$.

C. From $\tilde{Z}(\lambda)$ to $p(s)$

In Refs. [19,29] we examined various choices for the elastic kernel $\bar{\epsilon}_k$, computed $\tilde{Z}(\lambda)$ for each choice, and extracted the scaled avalanche distribution $p(s)$. Here we show that $p(s)$ can directly be written as a function of $\bar{\epsilon}_k$, or $e(p)$.

1. General formalism

The definition Eq. (75) implies

$$\int_0^\infty ds sp(s) e^{\lambda s} = \tilde{Z}'(\lambda). \quad (86)$$

While $p(s)$ does not admit a Laplace transform, the function $sp(s)$ does. Laplace inversion then yields

$$\begin{aligned} sp(s) &= \frac{1}{2i\pi} \int_{-i\infty}^{i\infty} d\lambda e^{-\lambda s} \tilde{Z}'(\lambda) \\ &= \frac{1}{2i\pi} \int_{-i\infty}^{i\infty} dZ e^{-s(Z-Z^2-\alpha J(Z))}, \end{aligned} \quad (87)$$

up to terms of order α^2 . At this stage there is a heuristic step, to go from the λ to the Z contour. We assume that the contour $Z = ix$ with $x \in \mathbb{R}$ is the correct one, as it is for the mean-field case ($\alpha = 0$) around which we perturb. We will check this result on known cases below. Then one has

$$\begin{aligned} sp(s) &= \frac{1}{2\pi} \int_{-\infty}^{\infty} dx e^{-isx - sx^2 + s\alpha J(ix)} \\ &= sp_{\text{MF}}(s) + \frac{\alpha s}{2\pi} \int_{-\infty}^{\infty} dx J(ix) e^{-isx - sx^2} \end{aligned} \quad (88)$$

to lowest order in α . We have introduced the scaled mean-field avalanche-size distribution, i.e., Eq. (87) at $\alpha = 0$,

$$p_{\text{MF}}(s) = \frac{1}{2\sqrt{\pi}} s^{-3/2} e^{-s/4}. \quad (89)$$

For the elastic manifold, it holds for $d \geq d_c$. We want to compute the correction to $sp(s)$ of order α , i.e., of order $\epsilon = d_c - d$:

$$\begin{aligned} &\frac{s}{2\pi} \int_{-\infty}^{\infty} dx J(ix) e^{-isx - sx^2} \\ &= \frac{1}{\epsilon \int_k \bar{\epsilon}_k^{-2}} \frac{s}{2\pi} \int_0^\infty dt \int_k \int_{-\infty}^{\infty} dx [te^{-t(\bar{\epsilon}_k - 2ix)} \partial_y^2 \\ &\quad + e^{-t(\bar{\epsilon}_k - 2ix)} \partial_y - e^{-t\bar{\epsilon}_k} \partial_y - 3te^{-t\bar{\epsilon}_k} \partial_y^2] e^{-isx - sx^2 + iyx} \Big|_{y=0} \\ &= \frac{1}{\epsilon \int_k \bar{\epsilon}_k^{-2}} \frac{s}{2\pi} \int_0^\infty dt \int_k \int_{-\infty}^{\infty} dx x e^{-\bar{\epsilon}_k t - isx - sx^2} \\ &\quad \times [e^{2itx}(i - tx) + 3tx - i]. \end{aligned} \quad (90)$$

The integrand behaves (before integration over x and k) as t^2 at small t as a result of the counterterms. It is useful to introduce the *elastic generating function*,

$$\mathcal{C}(t) := \frac{1}{\epsilon \int_k \bar{\epsilon}_k^{-2}} \int_k e^{-t\bar{\epsilon}_k} = \frac{1}{C_\beta} \int_p e^{-te(p)}, \quad (91)$$

in terms of which we get, integrating Eq. (90) over x :

$$\frac{p(s)}{p_{\text{MF}}(s)} = 1 + \alpha \frac{1}{4s} \int_0^\infty dt \mathcal{C}(t) X(t, s) \quad (92)$$

$$X(t,s) = e^{t-t^2/s} [4t^3 + s^2(2+t) - 2st(3+2t)] - s[2s + 3t(s-2)]. \quad (93)$$

This is our final and most general formula, valid for any elasticity ϵ_k and to first order in α , i.e., in ϵ . By performing the integral over s , one checks that it satisfies automatically the two normalization conditions for $p(s)$ (to order α).

2. Special cases

We now check that this formula recovers previous known results.

a. Standard local elasticity. For $\epsilon_k = Kk^2 + m^2$ one has $\beta = 2$ and $e(p) = p^2 + 1$. Using that $\int_k e^{-ik^2} = (4\pi)^{-d/2} t^{-d/2}$ and computing the momentum integral in $d = d_c = 4$, one finds

$$C(t) = \frac{1}{2t^2} e^{-t}. \quad (94)$$

Inserting into Eq. (92) and performing the t integral yields

$$\frac{p(s)}{p_{\text{MF}}(s)} = 1 + \frac{\alpha}{16} [(\ln s + \gamma_E)(s-6) + 4s - 8\sqrt{\pi}\sqrt{s} + 4], \quad (95)$$

which recovers the result (169) of [29] (to lowest order in α).

b. Elasticity of flat contact line and generalization. From Eq. (63) the elasticity of a flat contact line $\varphi + \theta = \pi/2$ is $\epsilon_k = \gamma \sin^2 \theta \sqrt{k^2 + \kappa^2}$. This gives:

$$\beta = 1, \quad K = \gamma \sin^2 \theta, \quad m^2 = \mu = K/\kappa \quad (96)$$

$$e(p) = \sqrt{p^2 + 1}. \quad (97)$$

It is instructive to slightly generalize this, and study

$$e(p) = \sqrt{p^2 + (1-a)^2} + a \quad (98)$$

with $0 < a < 1$, which interpolates between the flat contact line for $a=0$ and $e(p) = |p| + 1$ for $a=1$, two cases studied in Ref. [29]. From the definition Eq. (91), computing the integral in $d = d_c = 2$, we obtain

$$C(t) = \frac{e^{-t}}{t^2} [1 + (1-a)t]. \quad (99)$$

Inserting into Eq. (92) and performing the t integral yields

$$\begin{aligned} \frac{p(s)}{p_{\text{MF}}(s)} = 1 + \frac{\alpha}{8} \{ & 16 - 12a - 6\gamma_E + (1-a)\sqrt{\pi}s^{3/2} \\ & + [(3-2a)s - 6]\ln s - 4(3-a)\sqrt{\pi}\sqrt{s} \\ & + s(2a(5-\gamma_E) + 3(\gamma_E - 2)) \}. \end{aligned} \quad (100)$$

For $a=0$, this is the same as (E14) of [29], and for $a=1$ has the same form as Eq. (95) upon a rescaling of α by a factor of 2, as noted in Ref. [29].

To obtain nicer forms for $p(s)$, and more convenient for extrapolations in physical dimension, one needs to re-exponentiate these direct ϵ expansion results, as done in Ref. [29]. We will not attempt to do this here for the general case.

D. More on the generating function $\tilde{Z}(\lambda)$

$\tilde{Z}(\lambda)$ is easier to compare with numerical and experimental data than the disorder distribution $p(s)$, since even if their statistics is mediocre averages over all data are taken, thus the statistical fluctuations are less pronounced. Therefore, we come back to the general formula and some examples.

1. Generating function in the general case

Since we work to the first order in α , i.e., in $\epsilon = d_c - d$ we can write:

$$\tilde{Z}(\lambda) = \frac{1}{2} (1 - \sqrt{1-4\lambda}) + \alpha \left. \frac{J\left(\frac{1}{2}[1 - \sqrt{1-4\lambda}]\right)}{\sqrt{1-4\lambda}} \right|_{z=Z_{\text{MF}}(\lambda)}. \quad (101)$$

up to higher order terms, hence we only need to compute the function $J(z)$ in Eq. (78) at the point of the mean field solution $z = Z_{\text{MF}}(\lambda) = \frac{1}{2}(1 - \sqrt{1-4\lambda})$.

The integral $J(z)$ can be rewritten using the elastic generating function $C(t)$ defined in Eq. (91) for an arbitrary elastic kernel ϵ_k as

$$J(z) = \int_0^\infty dt C(t) [e^{2tz}(tz^2 + z) - z - 3tz^2]. \quad (102)$$

2. Standard elasticity

Standard elasticity has the form $e(p) = p^2 + 1$ and using Eq. (94) one finds:

$$J(z) = \frac{1}{2} z [2z + (1-3z)\log(1-2z)]. \quad (103)$$

This result is in agreement with Eq. (150) of [29]. The value of α to be used in Eq. (101) for extrapolation to $d=1$ (i.e., $\epsilon=3$) is $\alpha = -2/3$.

3. Flat contact line and generalization

From the form $e(p) = \sqrt{p^2 + (1-a)^2} + a$ and using Eq. (99) one finds

$$J(z) = z \left[\frac{2z(a+z-3az)}{1-2z} + (a-3z)\log(1-2z) \right]. \quad (104)$$

This agrees with (E10) of [29] for $a=0$ and with Eq. (103) up to a global factor of 2, as predicted in [29]. The value of α to be used in Eq. (101) for extrapolation to $d=1$ (i.e., $\epsilon=1$) is $\alpha = -2/9$.

4. Contact line for arbitrary angles θ and φ

Having tested our general formula on the known cases we can now apply them to the case of the elastic kernel Eq. (62). Let us specify the relevant parameters and functions. For the contact line $\beta=1$, $d_c=2$, and

$$m^2 = \mu = \epsilon_{q=0} = \frac{\gamma\kappa}{t} \sin \theta \cos \varphi, \quad (105)$$

$$K = \gamma \sin^2 \theta, \quad (106)$$

$$\kappa = \frac{1}{L_c} = \sqrt{\frac{\rho g}{\gamma}}, \quad t = \sqrt{\frac{\sin(\theta + \varphi) + 1}{2}}, \quad (107)$$

$$\tilde{\epsilon}_q = e(p) = \tilde{e}(r) = 1 + \frac{(r^2 - 1)[t(r + t) + 1] \sin \theta}{(r^2 + 3rt + 3t^2 - 1) \cos \varphi}, \quad (108)$$

$$r = \sqrt{1 + \frac{q^2}{\kappa^2}} = \sqrt{1 + \frac{\cos^2 \varphi}{t^2 \sin^2 \theta} p^2}, \quad p = \frac{K}{\mu} q. \quad (109)$$

We have defined for convenience a new function $\tilde{e}(r)$ since r is the implicit variable in the final formula. Note that for the flat interface $\theta + \varphi = \pi/2$, one recovers $\tilde{e}(r) = r$.

The generating function $\tilde{Z}(\lambda)$ for the contact line can, thus, be computed from Eq. (101) using Eq. (85) and performing the integral in dimension $d_c = 2$. Upon a change of variable we get:

$$J(z) = \frac{t^2 \sin^2 \theta}{\cos^2 \varphi} \times \int_1^\infty dr r \left[\frac{z^2}{[\tilde{e}(r) - 2z]^2} + \frac{z}{\tilde{e}(r) - 2z} - \frac{z}{\tilde{e}(r)} - 3 \frac{z^2}{\tilde{e}(r)^2} \right]. \quad (110)$$

Performing this integral analytically, or even the one involved in computing $\mathcal{C}(t)$, is rather awkward, and we have preferred to use numerical integration.

To relate to the experiment of [6], we have computed $J(z)$ numerically for $\theta = 40^\circ$, $\varphi = 0^\circ$. We give some explicit values: $J(-1/2) = -0.493277$, $J(-1) = -3.10539$, $J(-3/2) = -8.79405$, and $J(-2) = -18.1329$. From this, we have computed and plotted $\tilde{Z}(\lambda)$ in Fig. 9, using the extrapolation to $\epsilon = 1$ in the one-loop result, i.e., using Eq. (101) with $\alpha = -2/9$. This is compared to the result of the scaled kernel $e(p) = \sqrt{p^2 + 1}$. The experimental data are also plotted on Fig. 9. Note that using the correct elasticity allows to get closer to the experimental data than using $e(p) = \sqrt{p^2 + 1}$, which is the kernel for the flat interface, and the only one previously available in the literature. Clearly, some discrepancy remains, which may be overcome by adding two-loop corrections, if the problem does not lay on the experimental side. However, what the plot shows unambiguously is that the results are *very sensitive* to the precise form of the elastic kernel, and using an approximation as $\tilde{\epsilon}_q = \sqrt{1 + q^2/\kappa^2}$ will never lead to agreement with experiment.

E. Local statistics of avalanches

1. Basic definitions

It is also possible to study in experiments the statistics of the avalanches occurring within a given portion of the elastic object, e.g., of the contact line. One thus defines the size of a

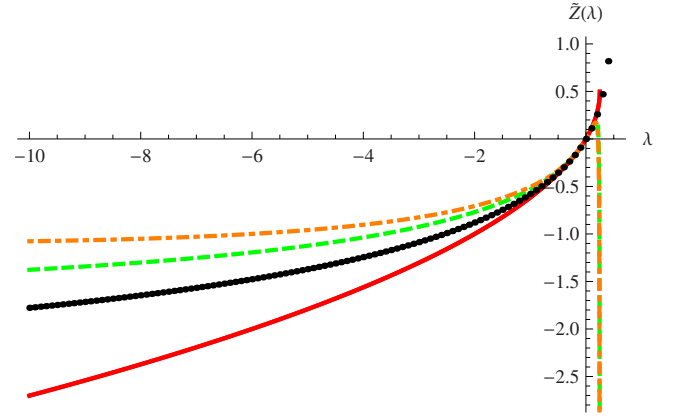


FIG. 9. (Color online) The generating function $\tilde{Z}(\lambda)$ of avalanche sizes as defined in Eq. (75). The curves are from bottom to top: Red/solid: mean-field result. Black dots: The experimental data of [6]. Dashed/green: Eq. (110) integrated numerically with the correct elasticity kernel (109) for $\theta = 40^\circ$, $\varphi = 0^\circ$. Dot-Dashed/orange: The same with the elastic kernel for $\theta = 90^\circ$, $\varphi = 0^\circ$, $\tilde{\epsilon}_q = \sqrt{1 + q^2/\kappa^2}$.

local avalanche, weighted by a characteristic function $\phi(x)$, e.g., a δ -distribution localized at $x=0$, as [39]:

$$S^\phi := \int_0^L d^d x \phi(x) [u_w^+(x) - u_w^-(x)] = \int_0^L d^d x \phi(x) [h_w^+(x) - h_w^-(x)]. \quad (111)$$

In [29], we have shown how the characteristic function

$$Z^\phi(\lambda) := \frac{1}{\langle S^\phi \rangle} \langle e^{\lambda S^\phi} - 1 \rangle \quad (112)$$

as well as the distribution of sizes can be computed within mean-field theory, valid at and above the upper critical dimension d_c . Since it already required some quite involved instanton calculus, we did not attempt to perform the ϵ expansion. Here we will perform the ϵ expansion, to one loop $\mathcal{O}(\epsilon)$, not on the full distribution, but on a simpler quantity, the second moment. More precisely, we will compute the universal amplitude ratio between the second global and local moments, quantities easily accessible in experiments and numerics. In fact, it was already measured in [20] in the case of standard local elasticity and the present analytical result was quoted. Here, we provide the details of the calculation and predict this ratio for the contact line which has not yet been measured.

2. Universal amplitude ratios between global and local avalanches: general formulation

Analogous to Eq. (71), we can define the scale of local avalanches as

$$S_m^\phi := \frac{\langle (S^\phi)^2 \rangle}{2 \langle S^\phi \rangle}. \quad (113)$$

From Eq. (F12) and (196) in [29] one has the general exact relation:

$$S_m^\phi = - \frac{1}{\int_x \phi(x)} \partial_w \int_{xyz'} \phi(y) \phi(x) g_{xz} g_{yz'} \Delta_{zz'}[w] \Big|_{w=0^+},$$

where $g_{xy} = \int_q e^{iq(x-y)} \epsilon_q^{-1}$ and $\Delta_{zz'}[w] = -R''_{zz'}[w]$ is the functional derivative taken at a uniform $w_t = w$ of the functional $R[w]$ (see e.g., [17,29] for its definition), the limit $w=0^+$ being taken at the end. For $\phi(x)=1$, using $\int_{zz'} \Delta_{zz'}[w] = L^d \Delta'(w)$ one recovers

$$S_m = \frac{\langle S^2 \rangle}{2\langle S \rangle} = -m^{-4} \Delta'(0^+). \quad (114)$$

Here we use the notations of Sec. II so that $m^2 = \epsilon_{k=0}$.

We can now use the results of the ϵ -expansion [30–32], or its first-principle derivation in formula (463) of [33]:

$$\Delta_{zz'}[w] = \delta_{zz'} \Delta(w) - \left(g_{zz'}^2 - \delta_{zz'} \int_t g_t^2 \right) \Delta'(w)^2 + \mathcal{O}(\epsilon^3).$$

Hence one obtains the ratio

$$\begin{aligned} a_\phi &:= \frac{S_m^\phi}{S_m} \\ &= \frac{m^4}{\int_x \phi(x)} \int_{xyz'} \phi(y) \phi(x) g_{xz} g_{yz'} \\ &\quad - 2m^4 \Delta''(0^+) \frac{1}{\int_x \phi(x)} \\ &\quad \times \int_{xyz'} \phi(y) \phi(x) g_{xz} g_{xz'} \left(g_{zz'}^2 - \delta_{zz'} \int_t g_t^2 \right) + \mathcal{O}(\epsilon^2), \end{aligned} \quad (115)$$

a formula valid for any function $\phi(x)$.

We now study avalanches which occur on a given subspace of co-dimension d' , defined by $x_\perp = 0$, i.e., of dimension $d_\phi = d - d'$, of the d -dimensional manifold, i.e., we choose

$$\phi(x) = \eta \delta^{d'}(x_\perp). \quad (116)$$

η will be specified later. The above formula leads to

$$\begin{aligned} a_\phi &= m^4 \eta I_2(d') + 2m^4 \eta [I_2(d) I_2(d') - I_A(d, d')] \Delta''(0) + \dots \\ &= m^4 \eta I_2(d') \left\{ 1 + \frac{2\tilde{\Delta}''(0)}{\epsilon} \left[1 - \frac{I_A(d, d')}{I_2(d) I_2(d')} \right] \right\} + \dots \end{aligned} \quad (117)$$

using the definition Eq. (83) of the rescaled disorder, $\tilde{\Delta}''(0) = \Delta''(0) \epsilon I_2(d)$, and defining the integrals

$$I_2(d) := \langle \text{bubble} \rangle = \int \frac{d^d q}{(2\pi)^d} \frac{1}{\epsilon_q^2} \quad (118)$$

$$I_A(d, d') := \langle \text{triangle} \rangle = \int \frac{d^{d'} k}{(2\pi)^{d'}} \frac{d^d q}{(2\pi)^d} \frac{1}{\epsilon_k^2} \frac{1}{\epsilon_q} \frac{1}{\epsilon_{k+q}}. \quad (119)$$

Note that in the last integral the momentum in the upper bubble runs over a space of dimension $d' < d$.

To perform the ϵ expansion we now use the scaling form Eq. (81) of the elastic kernel. This yields to zeroth and first order in $\epsilon = d_c - d$:

$$a_\phi = \eta \mu^{d'} K^{-d'/\beta} \tilde{I}_2(d') \left\{ 1 + \frac{2\tilde{\Delta}''(0)}{\epsilon} \left[1 - \frac{\tilde{I}_A(d, d')}{\tilde{I}_2(d) \tilde{I}_2(d')} \right] \right\} + \dots \quad (120)$$

in terms of the dimensionless integrals

$$\tilde{I}_2(d) := \langle \text{bubble} \rangle = \int \frac{d^d q}{(2\pi)^d} \frac{1}{e(q)^2}, \quad (121)$$

$$\tilde{I}_A(d, d') := \langle \text{triangle} \rangle = \int \frac{d^{d'} k}{(2\pi)^{d'}} \frac{d^d q}{(2\pi)^d} \frac{1}{e(k)^2} \frac{1}{e(q)} \frac{1}{e(k+q)}. \quad (122)$$

To obtain a meaningful amplitude we now make the choice

$$\eta = \left(\frac{K^{1/\beta}}{\mu} \right)^{d'}. \quad (123)$$

Note that comparing with experiments then requires a precise knowledge of the internal length scale $K^{1/\beta}/\mu$ defined by the (renormalized) mass $m^2 = \mu^\beta$ and elastic constant $K = \lim_{q \gg \kappa} \epsilon_q/q^\beta$. Alternatively, it may be used as a method to measure this length.

3. Standard local elasticity

We now specify to standard elasticity $\epsilon_k = Kk^2 + m^2$, i.e., $\beta=2$, $d_c=4$ and $e(p) = p^2 + 1$. We study $d'=1$.

We need the integrals:

$$\tilde{I}_2(d) = \Gamma\left(2 - \frac{d}{2}\right) (4\pi)^{-d/2} \quad (124)$$

$$\tilde{I}_2(d'=1) = \int \frac{dq}{2\pi} \frac{1}{(q^2 + 1)^2} = \frac{1}{4} \quad (125)$$

$$\frac{\tilde{I}_A(d, d')}{\tilde{I}_2(d) \tilde{I}_2(d')} - 1 = \frac{I}{\tilde{I}_2(d) \tilde{I}_2(d')} \quad (126)$$

This involves the integral

$$\begin{aligned} I &= \int \frac{dk}{2\pi} \frac{1}{(k^2 + 1)^2} \int \frac{dq}{2\pi} \frac{d^{d-1} p}{(2\pi)^d} \\ &\quad \times \left[\frac{1}{[(k+q)^2 + p^2 + 1](q^2 + p^2 + 1)} - \frac{1}{(q^2 + p^2 + 1)^2} \right] \end{aligned} \quad (127)$$

The calculation of this integral is performed in Appendix. To

the order ϵ we are working, we only need to compute it in $d=d_c=4$. We find

$$I = (4\pi)^{-5/2} \Gamma\left(\frac{3}{2}\right) \left[4 + \frac{2}{9}(7\sqrt{3} - 18)\pi \right]. \quad (128)$$

Putting all these results together we obtain

$$\begin{aligned} a_\phi &= \frac{1}{4} + \alpha \left(1 - \pi + \frac{7\pi}{6\sqrt{3}} \right) + \mathcal{O}(\epsilon^2) \\ &= 0.25 - 0.025\,493\,4\alpha + \mathcal{O}(\epsilon^2) \end{aligned} \quad (129)$$

with $\alpha = -\frac{\epsilon}{3}(1 - \zeta_1)$. This is the expansion for a manifold with co-dimension one in $\epsilon=4-d$.

For the one-dimensional string, simulated in [20], we need to extrapolate to $\epsilon=3$ which yields $\alpha=-2/3$. The two possible Padé expansions are

$$\frac{1}{a_\phi} = \frac{1}{\frac{1}{4} + 0.016\,995\,6} = 3.74538, \quad (130)$$

$$\frac{1}{a_\phi} = 4 - 16\alpha \left[1 + \left(\frac{7}{6\sqrt{3}} - 1 \right) \pi \right] = 3.72807. \quad (131)$$

Hence, an estimate of the ratio is

$$\frac{1}{a_\phi} = 3.74 \pm 0.01. \quad (132)$$

Another expansion is the expansion in fixed dimension in powers of $\tilde{\Delta}$. It is likely to be less precise than the ϵ expansion, but being simpler in spirit we indicate here its prediction. One evaluates directly the integrals in $d=d'=1$. Using the results from the Appendix, this yields

$$a_\phi = \frac{1}{4} \left[1 + \frac{2\tilde{\Delta}''(0^+)}{9\epsilon} + \dots \right], \quad (133)$$

and inserting the one-loop value $\tilde{\Delta}''(0^+) = -\alpha = \frac{2}{9}\epsilon$ we find the estimate $1/a_\phi \approx 3.81$, slightly larger than Eq. (132).

4. Contact-line elasticity

For the contact-line elasticity, the $\epsilon=2-d$ expansion can be done as indicated above. As it requires performing two-dimensional integrals we will only give here the fixed-dimension estimate for $d=d'=1$, which requires only a one-dimensional integral on each momentum. We further perform them numerically using the form Eq. (109). We give two examples:

(i) flat interface $\varphi + \theta = \pi/2$.

Then $e(p) = \sqrt{p^2 + 1}$ and we obtain

$$\tilde{I}_2(1) = \frac{1}{2}, \quad (134)$$

$$2 \left[1 - \frac{\tilde{I}_A(1,1)}{\tilde{I}_2(1)\tilde{I}_2(1)} \right] \approx 0.312\,811\dots \quad (135)$$

This yields

$$a_\phi = \frac{1}{2} \left(1 + 0.312\,811\frac{2}{9} + \dots \right) \quad (136)$$

and $1/a_\phi \approx 1.87$.

(ii) experiments of Ref. [6], i.e., $\varphi=0^\circ$, $\theta=40^\circ$:

We find

$$\tilde{I}_2(1) \approx 0.41867, \quad (137)$$

$$2 \left[1 - \frac{\tilde{I}_A(1,1)}{\tilde{I}_2(1)\tilde{I}_2(1)} \right] \approx 0.333\,101\dots \quad (138)$$

This yields

$$a_\phi = 0.41867 \left(1 + 0.333\,101\frac{2}{9} + \dots \right) \quad (139)$$

and $1/a_\phi \approx 2.22$, whereas the mean-field approximation is $1/a_\phi^{\text{MF}} \approx 2.39$.

It is interesting to note that the ‘‘elastic length’’ $\eta = K/\mu$ which enters the definition Eqs. (111) and (116) of S^ϕ and a_ϕ reads:

$$\eta = \frac{K}{\mu} = L_c \frac{\sin \theta}{\cos \varphi} \sqrt{\frac{\sin(\theta + \varphi) + 1}{2}}, \quad (140)$$

i.e., it only involves the capillary length and geometric prefactors, thus, is well-known experimentally. In addition, one can measure the dependence of a_ϕ on the plate angle φ .

V. CONCLUSIONS

In this paper, we have reconsidered the problem of contact-line depinning. We have shown, that the usual DeGennes-Joanny form of the elastic energy $\mathcal{E}[h] = \frac{1}{2} \int \frac{dq}{2\pi} \epsilon_q |h_q|^2$, $\epsilon_q = \gamma \sqrt{q^2 + \kappa^2}$ is only an approximation for the case of a nonflat minimal energy surface, but has to be replaced by the more general expression Eq. (2).

In the second part of this paper, we have studied the consequences of a more general form of the elastic energy for the avalanche-size distribution at depinning, giving explicitly the results of a contact line. While the calculations are rather involved, the consequences can be summarized in a plot for the parameter-free generating function $\tilde{Z}(\lambda)$, see Fig. 9.

While agreement with experiments is certainly improved, differences remain. Part of these differences are due to experimental shortcomings, e.g., the size of defects may be reduced. On the theoretical side, improvements can come from higher-loop corrections, or from taking into account nonlinear elastic terms. While the latter have for some time been deemed necessary to account for the large roughness exponent [27], the latest experiments, i.e., those on which our comparison is based, suggest that this conclusion might be premature.

We have further discussed ‘‘local avalanches,’’ i.e., the jump-size distribution at a given point, which is different from the ‘‘global’’ avalanche-size distribution (distribution of swiped areas). These are further experimentally accessible observables, on which not much was known previously apart

from the tree-level results given in one special case in [29]. We have given here the results for the universal ratio $a_\phi = \frac{S_m^\phi}{S_m}$, where the typical scales of the local avalanche S_m^ϕ , and of the global avalanche S_m have been defined in Eqs. (113) and (114).

We hope that our results stimulate further experimental studies.

ACKNOWLEDGMENTS

It is a pleasure to thank Etienne Rolley and Alberto Rosso for stimulating discussions.

APPENDIX: STANDARD ELASTICITY: CALCULATION OF AN INTEGRAL

The integral defined in the text can be written as

$$\begin{aligned}
 I &= \int \frac{dk}{2\pi} \int \frac{dq}{2\pi} \frac{d^{d-1}p}{(2\pi)^d} \int_{t_1, t_2 > 0} t e^{-t(k^2+1)} \\
 &\quad \times \{e^{-t_1[(k+q)^2+p^2+1]+t_2(q^2+p^2+1)} - e^{-(t_1+t_2)(q^2+p^2+1)}\} \\
 &= (4\pi)^{-(d+1)/2} \int_{t_1, t_2 > 0} t(t_1+t_2)^{-(d-1)/2} \{(tt_1+tt_2+t_1t_2)^{-1/2} \\
 &\quad - [t(t_1+t_2)]^{-1/2}\} e^{-t-t_1-t_2}, \quad (\text{A1})
 \end{aligned}$$

using the general formula $\int_q e^{-q \cdot C \cdot q} = (4\pi)^{-d/2} (\det C)^{-1/2}$. Performing the changes of variables $t_1 \rightarrow tt_1$ and $t_2 \rightarrow tt_2$ yields

$$\begin{aligned}
 I &= (4\pi)^{-(d+1)/2} \int_0^\infty dt \int_0^\infty dt_1 \int_0^\infty dt_2 e^{-t(t_1+t_2+1)} \\
 &\quad \times t^{5/2-d/2} (t_1+t_2)^{1/2-d/2} \left[\frac{1}{\sqrt{t_2 t_1 + t_1 + t_2}} - \frac{1}{\sqrt{t_1 + t_2}} \right]. \quad (\text{A2})
 \end{aligned}$$

Integration over t yields

$$\begin{aligned}
 I &= (4\pi)^{-(d+1)/2} \int_0^\infty dt_1 \int_0^\infty dt_2 (t_1+t_2)^{1/2-d/2} (t_1+t_2+1)^{(d-7)/2} \\
 &\quad \times \Gamma\left(\frac{7}{2} - \frac{d}{2}\right) \left[\frac{1}{\sqrt{t_2 t_1 + t_1 + t_2}} - \frac{1}{\sqrt{t_1 + t_2}} \right]. \quad (\text{A3})
 \end{aligned}$$

Setting $t_1 = st$, $t_2 = (1-s)t$, one obtains

$$I = \frac{9\sqrt{3}2^d \Gamma\left(2 - \frac{d}{2}\right) {}_3F_2\left(\frac{1}{2}, 1, 2 - \frac{d}{2}; -\frac{1}{2}, \frac{3}{2}; \frac{1}{4}\right) + 2\sqrt{\pi}[9\sqrt{3}2^d - 4 \cdot 3^{d/2}(d+3)] \Gamma\left(\frac{3}{2} - \frac{d}{2}\right)}{4^{d+1} \pi^{d/2} 9\sqrt{3}} - 2^{-2-d} \pi^{-d/2} \Gamma\left(2 - \frac{d}{2}\right). \quad (\text{A7})$$

The combination $2\left[1 - \frac{\tilde{I}_A(d,1)}{\tilde{I}_2(1)\tilde{I}_2(d)}\right]$ is plotted on Fig. 10.

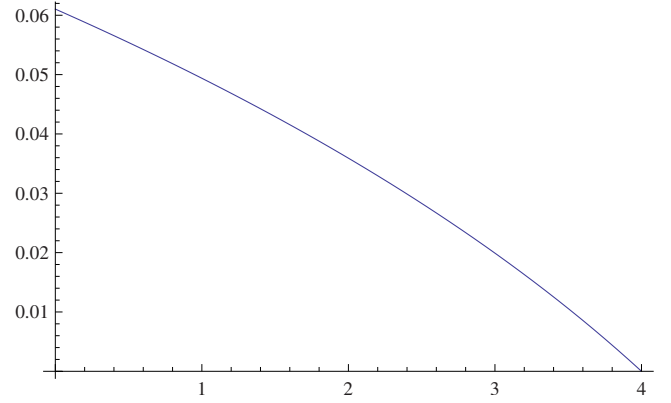


FIG. 10. (Color online) The combination $2\left[1 - \frac{\tilde{I}_A(d,1)}{\tilde{I}_2(1)\tilde{I}_2(d)}\right]$ as a function of d , for standard elasticity.

$$\begin{aligned}
 I &= (4\pi)^{-(d+1)/2} \int_0^\infty dt \int_0^1 ds t^{1-d/2} (t+1)^{(d-7)/2} \Gamma\left(\frac{7}{2} - \frac{d}{2}\right) \\
 &\quad \times \left[\frac{1}{\sqrt{1+(1-s)st}} - 1 \right] \\
 &= (4\pi)^{-(d+1)/2} \int_0^\infty dt t^{1-d/2} (t+1)^{(d-7)/2} \Gamma\left(\frac{7}{2} - \frac{d}{2}\right) \\
 &\quad \times \left[\frac{2}{\sqrt{t}} \operatorname{arccot}\left(\frac{2}{\sqrt{t}}\right) - 1 \right]. \quad (\text{A4})
 \end{aligned}$$

One can perform the integral directly in $d=1$, with the result

$$I = -\frac{1}{144}. \quad (\text{A5})$$

Thanks to the counterterm it also admits a limit for $d=4$:

$$I = \frac{1}{8\pi^2} \left[\frac{1}{2} + \frac{\pi}{36} (-18 + 7\sqrt{3}) \right]. \quad (\text{A6})$$

Finally the expression for any d is

- [1] G. Blatter, M. V. Feigel'man, V. B. Geshkenbein, A. I. Larkin, and V. M. Vinokur, *Rev. Mod. Phys.* **66**, 1125 (1994).
- [2] T. Nattermann and S. Scheidl, *Adv. Phys.* **49**, 607 (2000).
- [3] W. Kleemann, J. Rhensius, O. Petracic, J. Ferre, J. P. Jamet, and H. Bernas, *Phys. Rev. Lett.* **99**, 097203 (2007).
- [4] G. Durin and S. Zapperi, *Phys. Rev. Lett.* **84**, 4705 (2000).
- [5] S. Zapperi, P. Cizeau, G. Durin, and H. E. Stanley, *Phys. Rev. B* **58**, 6353 (1998).
- [6] P. Le Doussal, K. J. Wiese, S. Moulinet, and E. Rolley, *EPL* **87**, 56001 (2009).
- [7] S. Moulinet, C. Guthmann, and E. Rolley, *Eur. Phys. J. E* **8**, 437 (2002).
- [8] S. Moulinet, C. Guthmann, and E. Rolley, *Eur. Phys. J. B* **37**, 127 (2003).
- [9] S. Moulinet, A. Rosso, W. Krauth, and E. Rolley, *Phys. Rev. E* **69**, 035103 (2004); e-print [arXiv:cond-mat/0310173](https://arxiv.org/abs/cond-mat/0310173).
- [10] A. Prevost, E. Rolley, and C. Guthmann, *Phys. Rev. Lett.* **83**, 348 (1999).
- [11] A. Prevost, E. Rolley, and C. Guthmann, *Phys. Rev. B* **65**, 064517 (2002).
- [12] E. Rolley and C. Guthmann, *Phys. Rev. Lett.* **98**, 166105 (2007).
- [13] D. S. Fisher, *Phys. Rep.* **301**, 113 (1998).
- [14] L. Ponsou, D. Bonamy, and E. Bouchaud, *Phys. Rev. Lett.* **96**, 035506 (2006).
- [15] L. Ponsou, D. Bonamy, and E. Bouchaud, French Patent No. FR:2892811 (2007).
- [16] K. J. Wiese and P. Le Doussal, *Markov Processes Relat. Fields* **13**, 777 (2007).
- [17] P. Le Doussal, *EPL* **76**, 457 (2006).
- [18] P. Le Doussal and K. J. Wiese, *EPL* **77**, 66001 (2007).
- [19] P. Le Doussal, A. A. Middleton, and K. J. Wiese, *Phys. Rev. E* **79**, 050101(R) (2009).
- [20] A. Rosso, P. Le Doussal, and K. J. Wiese, *Phys. Rev. B* **80**, 144204 (2009).
- [21] J. F. Joanny and P. G. De Gennes, *J. Chem. Phys.* **81**, 552 (1984).
- [22] Y. Pomeau and J. Vannimenus, *J. Colloid Interface Sci.* **104**, 477 (1985).
- [23] V. S. Nikolayev and D. A. Beysens, *EPL* **64**, 763 (2003).
- [24] F. Brochard and P. G. De Gennes, *Langmuir* **7**, 3216 (1991).
- [25] A. Checco, *EPL* **85**, 16002 (2009).
- [26] R. Golestanian and E. Raphael, *EPL* **55**, 228 (2001).
- [27] P. Le Doussal, K. J. Wiese, E. Raphael, and R. Golestanian, *Phys. Rev. Lett.* **96**, 015702 (2006).
- [28] C. Bachas, P. Le Doussal, and K. J. Wiese, *Phys. Rev. E* **75**, 031601 (2007).
- [29] P. Le Doussal and K. J. Wiese, *Phys. Rev. E* **79**, 051106 (2009).
- [30] P. Chauve, P. Le Doussal, and K. J. Wiese, *Phys. Rev. Lett.* **86**, 1785 (2001).
- [31] P. Le Doussal, K. J. Wiese, and P. Chauve, *Phys. Rev. B* **66**, 174201 (2002).
- [32] P. Le Doussal, K. J. Wiese and P. Chauve, *Phys. Rev. E* **69**, 026112 (2004).
- [33] P. Le Doussal, *Ann. Phys. (N.Y.)* **325** (1), 49(R) (2010).
- [34] [21] introduce the capillary length L_c *ad hoc* as a cutoff for the contact-line profile in response to a δ -like force.
- [35] Note that height correlations decay with the capillary length. Thus, if one has a system which is much larger (in units of the capillary length) than the observation window, one will not see any finite size effects.
- [36] Note that the integration by part of ∂_y produces no surface term. This can be made rigorous considering a periodic modulation $h(y)$. We thus restrict here to functions that can be written as sum of periodic modulations, or have compact support.
- [37] In the experiment of Ref. [6], there is an additional slowly varying offset.
- [38] Statics means the following: If we could get the contact line to relax, and find its true minimal-energy configuration as a function of plate position—maybe by waiting hundred years—then we could take one snapshot every hundred years, and deduce the avalanche sizes from the snapshots. Our statement says that this statistics and the driven one would differ only at two-loop order.
- [39] Note that the variable $\phi(x)$ entering in S^ϕ and a^ϕ bears no relation to the plate angle φ introduced previously.